## Chapter 6 Appendix 2

# CALCULATION OF DOSES DUE TO ATOMIC BOMB INDUCED SOIL ACTIVATION

**Michael L. Gritzner and William A. Woolson**
*Science Applications International Corporation*

---

The Atomic bombs detonated over Hiroshima and Nagasaki emitted both prompt and delayed neutrons. Some of the neutrons entered the ground where they were captured and produced radioactive nuclides. Since there were relatively few high-energy neutrons available for fast-neutron activation at Hiroshima and even fewer at Nagasaki, most of these reactions in the ground were capture of thermal neutrons. The resulting radioisotopes subsequently decayed over time with half-lives ranging from several minutes to several years. The radioisotopes decayed by emitting gamma rays with a spectrum of energies. These gamma rays, attenuated by the ground, escaped into the air and produced a radiation field that lasted for years.

These gamma rays must be considered in determining the radiation doses of the survivors of the A-bombs. The kerma rates they produced proved to be small relative to those produced by the prompt and delayed radiations; however, their contribution had to be estimated to good accuracy for at least two reasons. First, the control group of survivors used in radiation risk studies was taken from those survivors located 2000 m or more from the hypocenter at the time of the bombing. The total free-field kerma in tissue at 2500 m from the hypocenter at Hiroshima was 1.2 rad. Some of these distant survivors were among the people who entered the devastated area after the explosion. Plausible scenarios can be produced for these people to have received similar doses from the gamma rays from the activated material. Thus there is a large uncertainty in their doses that must be understood before they are used as part of the control group. Second, comparison of soil activation computations with available measurements may help resolve current discrepancies between measurements and calculations of $^{60}$Co and $^{152}$Eu (see Chapter 5).

### Calculation of Soil Activation and Doses

The technique used to calculate the fluence of neutrons is described in Chapter 3. In brief, the spectral, spatial, and directional distributions of the prompt neutrons in the air and ground

Table 1. Composition for Calculation of Induced Soil Activation, Hiroshima and Nagasaki[a]

| Element | Hiroshima | Nagasaki |
|---|---|---|
| Na | 5.451E−4[b] | 2.556E−4 |
| Al | 2.061E−3 | 2.816E−3 |
| Si | 9.315E−3 | 6.806E−3 |
| P | 4.247E−6 | 2.424E−5 |
| K | 7.191E−4 | 1.150E−4 |
| Ca | 1.583E−4 | 2.267E−4 |
| Sc | 8.708E−8 | 3.483E−7 |
| Ti | 2.567E−5 | 1.034E−4 |
| Cr | 3.087E−7 | 2.289E−6 |
| Mn | 6.659E−6 | 1.796E−5 |
| Fe | 2.482E−4 | 8.247E−4 |
| Co | 4.916E−8 | 2.950E−7 |
| Ni | 6.668E−8 | 7.201E−7 |
| Cu | 4.436E−7 | 6.284E−7 |
| Mg | 8.180E−5 | 2.367E−4 |
| V | 3.428E−7 | 2.628E−6 |

[a]Atoms/barn $cm^3$
[b]Read as $5.451 \times 10^{-4}$

Table 2. Atomic Bomb Parameters, Hiroshima and Nagasaki

| Parameter | Hiroshima | Nagasaki |
|---|---|---|
| Height of Burst | 580 m | 503 m |
| Yield | 15 kt | 21 kt |
| Prompt Neutron Output | 2.655 moles | 5.742 moles |

were available from the two-dimensional, discrete-ordinates, air-over-ground calculations by Pace. These neutron spectra were multiplied by the activation cross sections[1] for those elements in the soil that result in radioactive isotopes that decay by photon emission and the product integrated over energy and direction. The soil composition used in these activation calculations is given in Table 1. The A-bomb parameters used are provided in Table 2. The result of the integration is a matrix of radioisotope concentrations in the soil at the time of the bomb bursts for different depths in the ground and for different distances from the hypocenter.

The next step was to calculate the transport of the source spectrum of gamma rays out of the ground at any given depth, time, and ground range. Since the number of possible sources (time, range, and depth dependent) was so very large, adjoint transport techniques were used for this part of the calculation. Specifically, an adjoint one-dimensional ANISN[2] calculation for a free-in-air tissue gamma-ray detector at 1 m above a flat plane of soil yields the relative importance of a source gamma ray of any energy at any depth in the ground to the kerma in tissue at the detector location. The free-field kerma at a given time and ground range was calculated by folding this adjoint importance function with the time-dependent gamma-ray spectrum for each of the radioisotopes and summing over all contributing radioisotopes.

The above discussion addresses the activation and the kerma resulting only from the prompt neutrons from the bomb. The contribution from delayed neutrons is not yet accounted for in the method. Neglecting the activation by delayed neutrons at Hiroshima is of little consequence since the kerma from the delayed neutrons is at most only 7% of that from the prompt neutrons. This is not true for Nagasaki. The situation at Nagasaki is unusual in that there were so few mid-to-high-energy prompt neutrons that the free-field kerma due to delayed neutrons is about 40% of the prompt neutron kerma out to 500 m ground range. Therefore, any estimate of the kerma from soil activation at Nagasaki must include that from delayed neutrons. The techniques used to calculate the delayed neutron contribution to the free-field kerma at the air/ground interface do not readily provide the energy and spatial distribution of the delayed neutrons in the ground. So we constructed a model to estimate the activation from delayed neutrons.

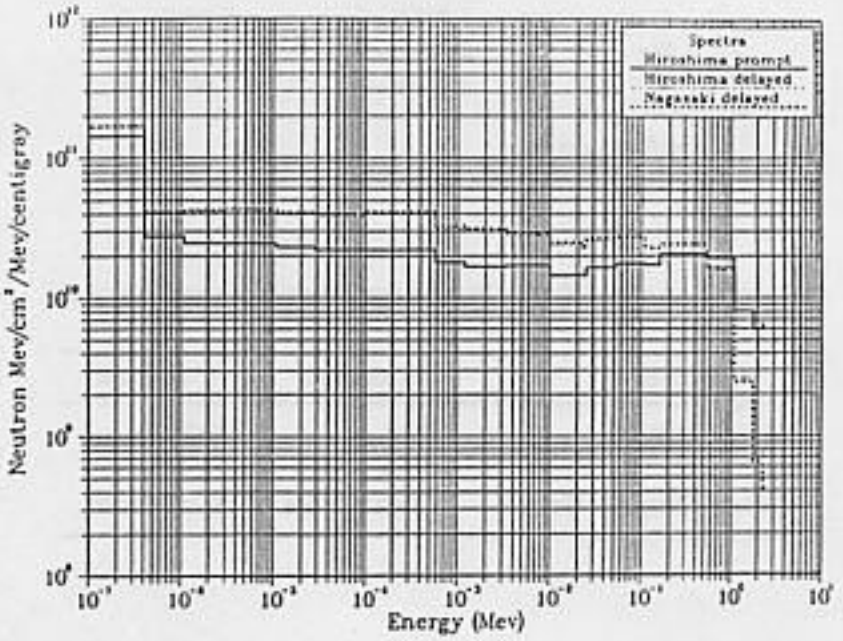


*Figure 1. Comparison of neutron spectra at 1 meter above ground Hiroshima and Nagasaki*

The three curves shown in Figure 1 reveal the interesting fact that the spectrum of delayed neutrons at Hiroshima and Nagasaki for a tissue detector at a height of 1 m is very similar to that of the prompt neutrons at Hiroshima for energies less than 2 MeV. Indeed, at Hiroshima the delayed and prompt neutron kermas versus ground range for ground ranges less than 700 m exhibit very nearly the same slope. Therefore, as a first approximation, the delayed neutron fluence distributions in the ground at Hiroshima and Nagasaki were synthesized as:

$$\phi_D\,(E,\,z,\,r) \;=\; \phi_p^H\,(E,\,z,\,r_o)\,\frac{K_D\,(r)}{K_p^H\,(r_o)} \qquad (1)$$

where:

$\phi_D(E,z,r)$ = the delayed neutron fluence as a function of energy E (less than 2 MeV), depth in the ground z, and ground range r;

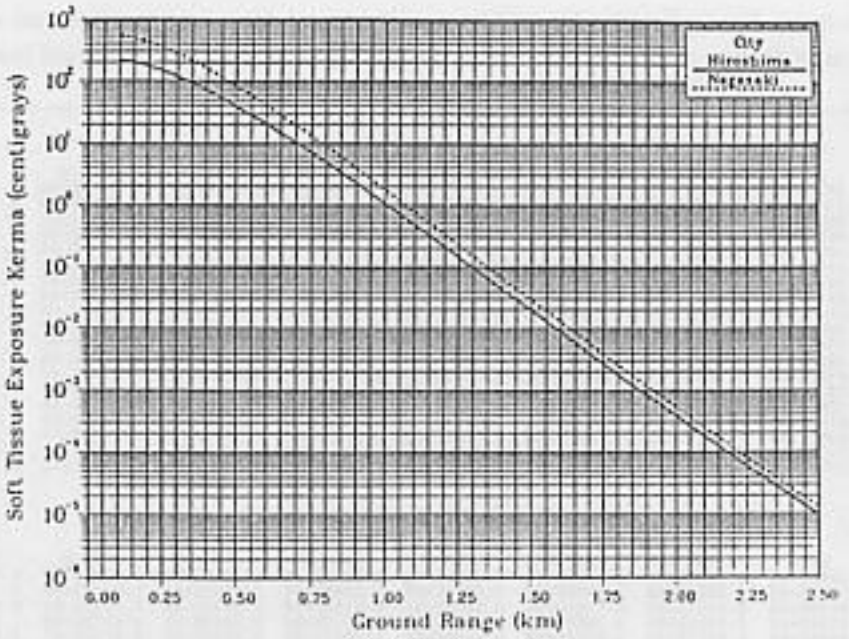


*Figure 2. Delayed neutron exposure kerma, Hiroshima and Nagasaki*

$\phi_p^H(E, z, r_o)$ = the prompt neutron fluence at Hiroshima as a function of energy E (less than 2 MeV), depth in the ground z, and at ground range $r_o$ = 700 m;

$K_D(r)$ = the delayed neutron soft tissue kerma for energies less than 2 MeV as a function of ground range r; and

$K_p^H(r_o)$ = the prompt neutron soft tissue kerma for energies less than 2 MeV at Hiroshima and at ground range $r_o$ = 700 m.

The assumption here is that the neutron spectra at 1 m above the ground is closely coupled to the spectra in the ground, particularly to that in the important first few centimeters. The delayed neutron kermas used, $K_D(r)$, are shown in Figure 2 for Hiroshima and Nagasaki. With these synthesized neutron distributions, the soil activation induced by delayed neutrons is treated exactly the same as for the prompt neutron contribution described earlier.

In summary, the energy and spatial prompt neutron fluence distributions in the ground from the state-of-the-art two-dimensional calculations together with synthesized delayed neutron fluence distributions in the ground are used to calculate the radioisotope concentrations at time zero, the time of the bombing. These are then folded with time and energy-dependent photon spectra and importance distributions to estimate kerma due to the soil activation at both Hiroshima and Nagasaki.

**Results of Calculations**

The result of the calculations just described is the free-in-air kerma in tissue due to gamma rays at 1 m above the ground as a function of ground range and time after the burst. These results are tabulated in Table 3 for both Hiroshima and Nagasaki. A plot of the kerma rate at ground zero versus time for each city is shown in Figure 3. The kerma rate is partitioned into three regimes, each of which is due principally to the decay of a single radioisotope. These

Table 3. Free-in-air Tissue Kerma due to Gamma Rays at 1 Meter Above Ground as a Function of Ground Range and Time After Bomb Burst, Hiroshima and Nagasaki (rad/hr)

15KT 580M HOB AT HIROSHIMA

| | GROUND RANGE | | | | | | | | | |
|---|---|---|---|---|---|---|---|---|---|---|
| TIME | 5 M | 50 M | 100 M | 200 M | 300 M | 500 M | 700 M | 1000 M | 1500 M | 2000 M |
| 0 SEC | 1.0322E+03 | 9.3435E+02 | 8.2157E+02 | 6.0256E+02 | 3.8620E+02 | 1.1384E+02 | 2.5106E+01 | 2.3177E+00 | 5.6723E-02 | 1.9718E-03 |
| 30 SEC | 8.5847E+02 | 7.7709E+02 | 6.8329E+02 | 5.0114E+02 | 3.2128E+02 | 9.4816E+01 | 2.0884E+01 | 1.9276E+00 | 4.7181E-02 | 1.6481E-03 |
| 6 MIN | 1.7515E+02 | 1.5855E+02 | 1.3941E+02 | 1.0225E+02 | 6.5534E+01 | 1.9183E+01 | 4.2614E+00 | 3.9344E-01 | 9.6368E-03 | 3.3531E-04 |
| 12 MIN | 3.4153E+01 | 3.0915E+01 | 2.7183E+01 | 1.9937E+01 | 1.2778E+01 | 3.7408E+00 | 8.3117E-01 | 7.6775E-02 | 1.8832E-03 | 6.5655E-05 |
| 30 MIN | 5.9718E+00 | 5.4058E+00 | 4.7521E+00 | 3.4858E+00 | 2.2333E+00 | 6.5338E-01 | 1.4585E-01 | 1.3365E-02 | 3.2588E-04 | 1.1225E-05 |
| 1 HR | 5.4667E+00 | 4.9478E+00 | 4.3501E+00 | 3.1901E+00 | 2.0441E+00 | 5.9784E-01 | 1.3264E-01 | 1.2202E-02 | 2.9529E-04 | 1.0126E-05 |
| 2 HR | 4.8444E+00 | 4.3844E+00 | 3.8548E+00 | 2.8269E+00 | 1.8113E+00 | 5.2978E-01 | 1.1753E-01 | 1.0812E-02 | 2.6149E-04 | 8.9644E-06 |
| 6 HR | 3.2977E+00 | 2.9845E+00 | 2.6239E+00 | 1.9242E+00 | 1.2329E+00 | 3.6063E-01 | 8.0027E-02 | 7.3645E-03 | 1.7822E-04 | 6.1126E-06 |
| 12 HR | 2.2084E+00 | 1.9913E+00 | 1.7507E+00 | 1.2838E+00 | 8.2262E-01 | 2.4063E-01 | 5.3405E-02 | 4.9161E-03 | 1.1892E-04 | 4.0836E-06 |
| 1 DAY | 1.1999E+00 | 1.0859E+00 | 9.5478E-01 | 7.0009E-01 | 4.4860E-01 | 1.3122E-01 | 2.9126E-02 | 2.6814E-03 | 6.4929E-05 | 2.2281E-06 |
| 3 DAY | 1.2791E-01 | 1.1575E-01 | 1.0178E-01 | 7.4624E-02 | 4.7817E-02 | 1.3988E-02 | 3.1046E-03 | 2.8583E-04 | 6.9219E-06 | 2.3754E-07 |
| 1 WK | 1.8885E-03 | 1.7092E-03 | 1.5027E-03 | 1.1020E-03 | 7.0613E-04 | 2.0654E-04 | 4.5832E-05 | 4.2173E-06 | 1.0216E-07 | 3.5015E-09 |
| 1 MO | 3.2142E-04 | 2.9102E-04 | 2.5591E-04 | 1.8769E-04 | 1.2027E-04 | 3.5166E-05 | 7.7958E-06 | 7.1761E-07 | 1.7380E-08 | 5.9598E-10 |
| 3 MO | 1.6814E-04 | 1.5214E-04 | 1.3465E-04 | 9.8761E-05 | 6.3284E-05 | 1.8503E-05 | 4.1021E-06 | 3.7672E-07 | 9.1611E-09 | 3.1414E-10 |
| 9 MO | 3.8722E-05 | 3.7888E-05 | 2.4450E-05 | 1.7932E-05 | 1.1491E-05 | 3.3604E-06 | 7.4542E-07 | 6.8583E-08 | 1.6668E-09 | 5.7621E-11 |
| 2 YR | 9.8788E-07 | 8.8115E-07 | 7.8261E-07 | 5.7371E-07 | 3.6792E-07 | 1.0865E-07 | 2.4217E-08 | 2.2925E-09 | 6.0359E-11 | 2.3944E-12 |
| 5 YR | 2.9553E-08 | 2.6488E-08 | 2.3218E-08 | 1.7001E-08 | 1.0921E-08 | 3.2363E-09 | 7.4075E-10 | 7.4052E-11 | 2.2198E-12 | 9.5378E-14 |
| 10 YR | 4.5989E-10 | 4.1155E-10 | 3.6089E-10 | 2.6482E-10 | 1.7088E-10 | 5.1552E-11 | 1.2218E-11 | 1.3238E-12 | 4.5215E-14 | 2.0625E-15 |
| 25 YR | 1.5216E-12 | 1.3777E-12 | 1.2332E-12 | 9.3292E-13 | 6.0188E-13 | 2.5971E-13 | 8.5178E-14 | 1.4688E-14 | 8.1249E-16 | 4.7313E-17 |

21KT 503M HOB AT NAGASAKI

| | GROUND RANGE | | | | | | | | | |
|---|---|---|---|---|---|---|---|---|---|---|
| TIME | 5 M | 50 M | 100 M | 200 M | 300 M | 500 M | 700 M | 1000 M | 1500 M | 2000 M |
| 0 SEC | 7.1843E+02 | 6.3343E+02 | 5.3601E+02 | 3.5773E+02 | 2.0946E+02 | 5.7426E+01 | 1.4031E+01 | 1.6185E+00 | 4.0887E-02 | 2.0188E-03 |
| 30 SEC | 5.9785E+02 | 5.2712E+02 | 4.4685E+02 | 2.9769E+02 | 1.7398E+02 | 4.7788E+01 | 1.1677E+01 | 1.3477E+00 | 4.1517E-02 | 1.6728E-03 |
| 6 MIN | 1.2271E+02 | 1.0819E+02 | 9.1554E+01 | 6.1104E+01 | 3.5711E+01 | 9.8104E+00 | 2.3973E+00 | 2.7677E-01 | 8.5315E-03 | 3.4482E-04 |
| 12 MIN | 2.4877E+01 | 2.1228E+01 | 1.7864E+01 | 1.1989E+01 | 7.0077E+00 | 1.9256E+00 | 4.7071E-01 | 5.4373E-02 | 1.6788E-03 | 6.7828E-05 |
| 30 MIN | 3.9854E+00 | 3.4958E+00 | 2.9577E+00 | 1.9737E+00 | 1.1531E+00 | 3.1657E-01 | 7.7313E-02 | 8.9154E-03 | 2.7411E-04 | 1.1027E-05 |
| 1 HR | 3.4416E+00 | 3.0339E+00 | 2.5667E+00 | 1.7126E+00 | 1.0002E+00 | 2.7436E-01 | 6.6936E-02 | 7.7038E-03 | 2.3566E-04 | 9.4254E-06 |
| 2 HR | 2.7794E+00 | 2.4502E+00 | 2.0730E+00 | 1.3833E+00 | 8.0793E-01 | 2.2162E-01 | 5.4065E-02 | 6.2215E-03 | 1.9022E-04 | 7.6033E-06 |
| 6 HR | 1.3287E+00 | 1.1646E+00 | 9.8553E-01 | 6.5792E-01 | 3.8445E-01 | 1.0553E-01 | 2.5753E-02 | 2.9639E-03 | 9.0659E-05 | 3.6257E-06 |
| 12 HR | 6.1277E-01 | 5.4847E-01 | 4.5755E-01 | 3.0565E-01 | 1.7872E-01 | 4.9118E-02 | 1.1988E-02 | 1.3803E-03 | 4.2246E-05 | 1.6988E-06 |
| 1 DAY | 2.7752E-01 | 2.4482E-01 | 2.0732E-01 | 1.3855E-01 | 8.1052E-02 | 2.2287E-02 | 5.4424E-03 | 6.2671E-04 | 1.9190E-05 | 7.6847E-07 |
| 3 DAY | 3.0899E-02 | 2.6553E-02 | 2.2485E-02 | 1.5027E-02 | 8.7908E-03 | 2.4173E-03 | 5.9026E-04 | 6.7975E-05 | 2.0815E-06 | 8.3351E-08 |
| 1 WK | 1.1283E-03 | 9.9456E-04 | 8.4123E-04 | 5.6108E-04 | 3.2755E-04 | 8.9705E-05 | 2.1902E-05 | 2.5215E-06 | 7.7198E-08 | 3.0899E-09 |
| 1 MO | 6.1195E-04 | 5.3921E-04 | 4.5583E-04 | 3.0375E-04 | 1.7715E-04 | 4.8487E-05 | 1.1822E-05 | 1.3608E-06 | 4.1648E-08 | 1.6667E-09 |
| 3 MO | 3.2662E-04 | 2.8778E-04 | 2.4327E-04 | 1.6211E-04 | 9.4552E-05 | 2.5885E-05 | 6.3124E-06 | 7.2670E-07 | 2.2262E-08 | 8.9175E-10 |
| 9 MO | 6.8671E-05 | 5.3448E-05 | 4.5187E-05 | 3.0120E-05 | 1.7579E-05 | 4.8197E-06 | 1.1769E-06 | 1.3579E-07 | 4.1833E-09 | 1.6875E-10 |
| 2 YR | 1.7692E-06 | 1.5578E-06 | 1.3197E-06 | 8.8452E-07 | 5.2289E-07 | 1.4659E-07 | 3.6499E-08 | 4.3451E-09 | 1.4489E-10 | 6.3855E-12 |
| 5 YR | 4.1129E-08 | 3.6097E-08 | 3.0817E-08 | 2.0975E-08 | 1.2762E-08 | 3.8858E-09 | 9.9245E-10 | 1.2853E-10 | 4.8861E-12 | 2.4583E-13 |
| 10 YR | 7.3535E-10 | 6.4746E-10 | 5.5620E-10 | 3.8808E-10 | 2.3626E-10 | 7.3309E-11 | 1.9839E-11 | 2.6902E-12 | 1.1681E-13 | 6.3245E-15 |
| 25 YR | 1.4835E-11 | 1.3267E-11 | 1.1867E-11 | 8.3538E-12 | 5.7157E-12 | 2.1817E-12 | 6.4970E-13 | 1.0563E-13 | 5.8883E-15 | 3.8224E-16 |

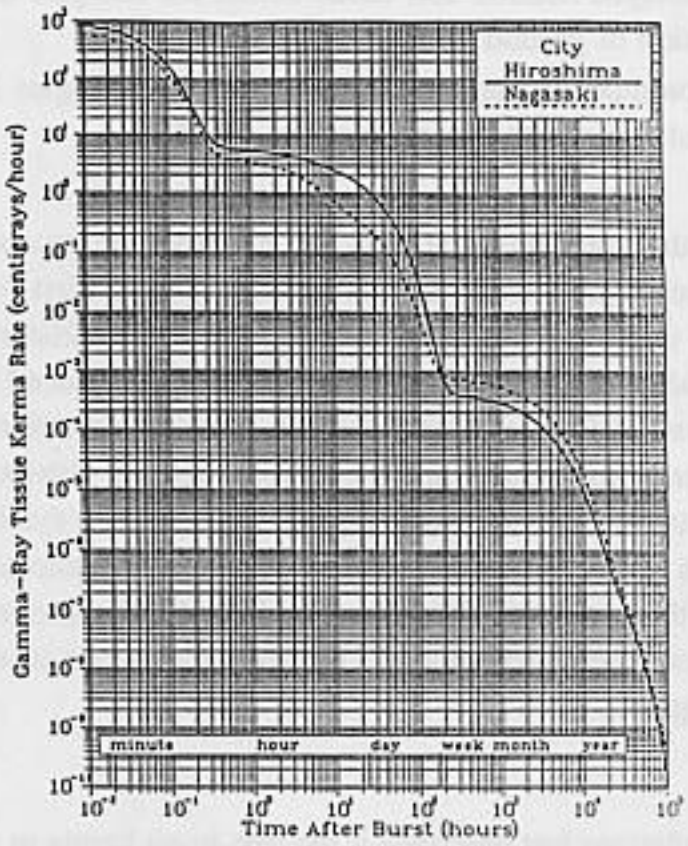


*Figure 3. Soil activation exposure kerma rate versus time after burst at ground zero, Hiroshima and Nagasaki*

fractional contributions to the tissue kerma rate from the important radioisotopes are shown in Figures 4 and 5 for Hiroshima and Nagasaki, respectively. Thermal neutron capture in $^{27}$Al creates the $^{28}$Al, which essentially completely decays after 30 minutes. About 20 minutes after the burst, the kerma rates begin to exhibit a difference between the two cities. The Hiroshima exposures are dominated by the $^{24}$Na radioisotope produced by thermal neutron capture in $^{23}$Na. This radioisotope dominates the kerma rate for almost a week after the explosion. At Nagasaki, however, thermal neutron capture in $^{55}$Mn, of which there is three times as much modeled in Nagasaki soil as in Hiroshima soil, creates $^{56}$Mn. The $^{56}$Mn dominates for about twice the 2.58 hour half-life before yielding to $^{24}$ Na with the 15.02-hour half-life. These different radioisotope contributors can be discerned in Figure 4 as the slightly flattened portion of the Nagasaki curve at about 10 hours after the burst. For the first week after the explosions, the calculated kerma rates are larger by factors of two to five at Hiroshima relative to Nagasaki. But at the end of the first week, the Nagasaki kerma rates become almost twice those at Hiroshima. The component radioisotopes are the same for each city, being $^{59}$Fe initially, followed by $^{46}$Sc. This marked reversal is merely a reflection of the two different ground compositions used. There is just over 3 times the iron and 10 times the amount of scandium in the Nagasaki soil relative to Hiroshima soil. Finally, beginning about two years after the burst, the much reduced kerma rates are due to the decay of $^{54}$Mn with a 7500 hour half-life. Since the radioisotopes produced at each city were created almost solely from thermal neutron capture, the data shown in Figures 3 to 5 for the hypocenter are applicable for all ground ranges, albeit with a different magnitude for the absolute kerma rates of Figure 3.

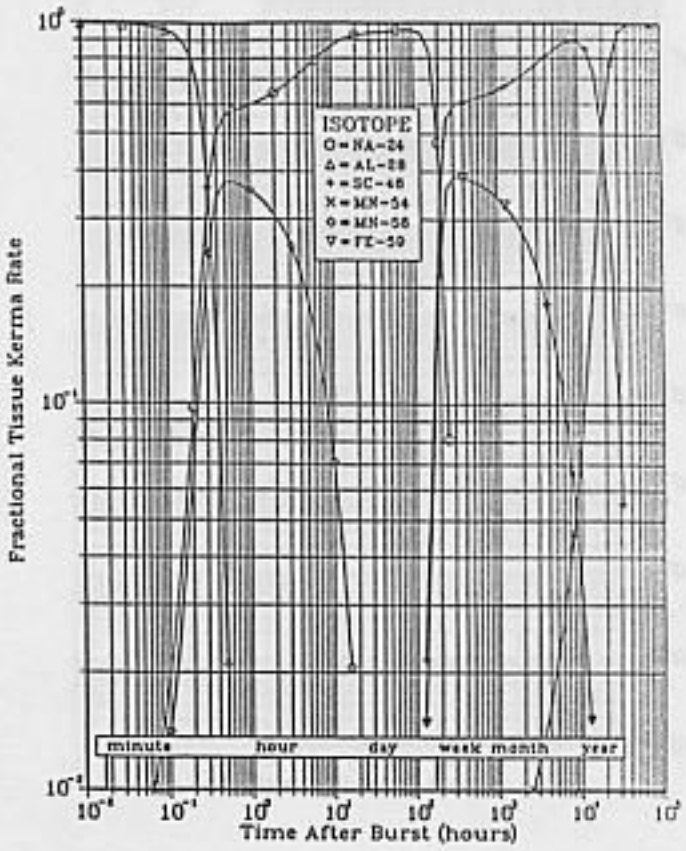


*Figure 4. Exposure kerma rate, isotopic components at ground zero, Hiroshima*

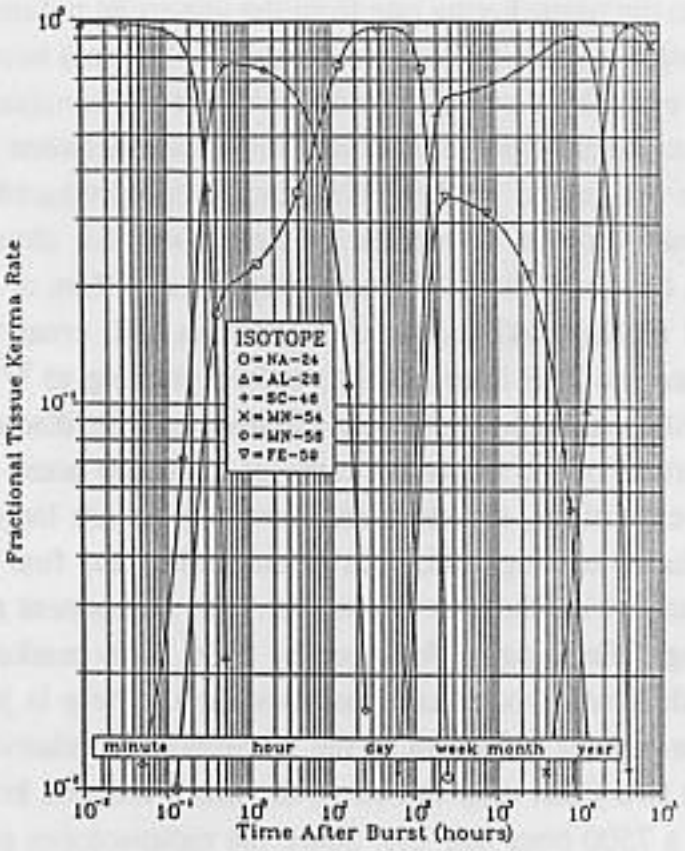


*Figure 5. Exposure kerma rate, isotopic components at ground zero, Nagasaki*

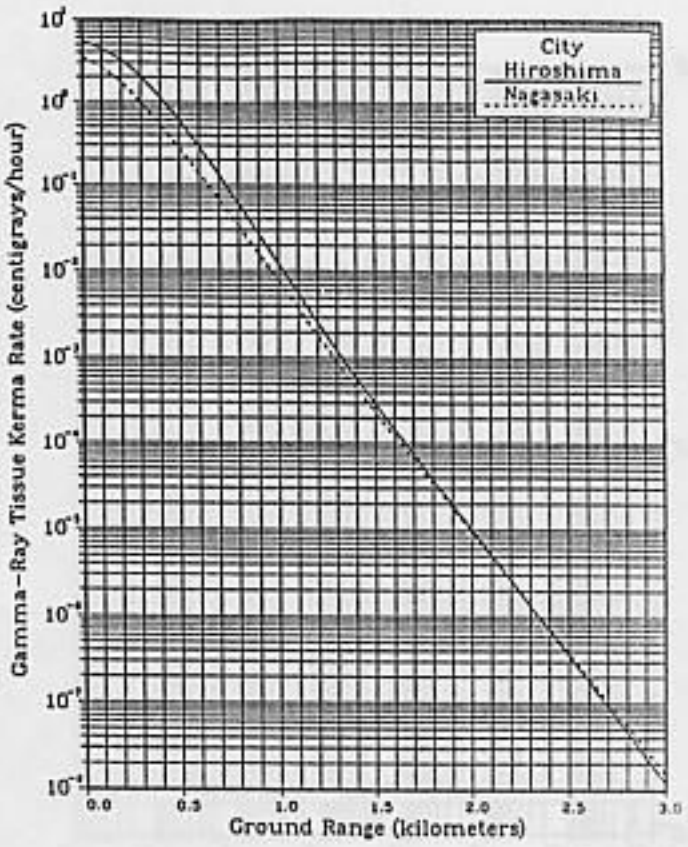


*Figure 6. Soil activation exposure kerma rate versus ground range at one hour after the bomb burst, Hiroshima and Nagasaki*

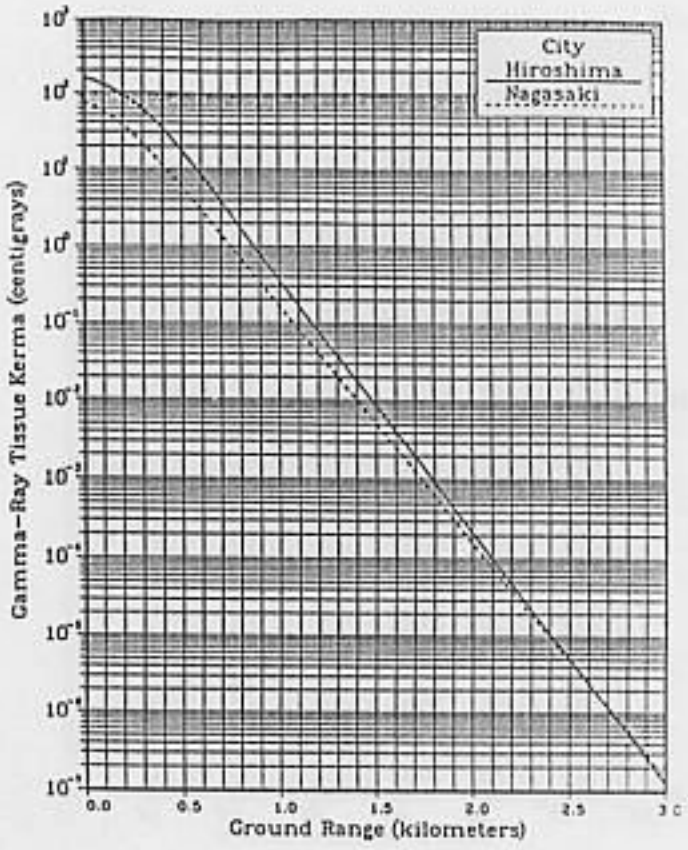


*Figure 7. Soil activation infinite exposure kerma versus ground range, Hiroshima and Nagasaki*

The free-field kerma rate variation with ground range from the hypocenters at one hour after the bursts is shown in Figure 6. The kerma rates shown beyond 2000 m were extrapolated from the 2000 m data. Since the radioisotopes were created principally by thermal neutron capture reactions, the curve for each city does not change shape for different times after the burst; the data in Figures 3 and 6 can be used to predict the kerma rate at any time up to $10^5$ hours after the burst at any ground range less than 3000 m. For example, to determine the kerma rate in Nagasaki at three days after the burst for a ground range of 1200 m, first determine the kerma rate at the hypocenter from Figure 3 as being about $3.0 \times 10^{-2}$ rad/h. Now, multiply this by the kerma rate at 1200 m from Figure 6 and divide by the kerma rate at the hypocenter from Figure 6 (i.e., the ratio $1.8\times 10^{-3} \div 3.4 = 5.29 \times 10^{-4}$). Thus, the predicted kerma rate is $3.0 \times 10 \times 5.29 \times 10^{-4} = 1.59 \times 10^{-5}$ rad/h.

Of interest also is an estimate of the kerma accumulated for both the A-bomb survivors and occupation forces. Its rigorous calculation would require a detailed time and spatial integration of these kerma rates for the subject's movements over a period of many months. Given the improbability of determining such information, the time integral for a stationary position can be estimated using the data shown in Figures 7 and 8. The two curves shown in Figure 7 show the kerma rate integrated over time from zero to infinity as a function of ground range for each city. The units of the integral are the rad accumulated for an infinite period of time after the burst. The curves shown in Figure 8 present the fraction of this infinite kerma at ground zero as a function of entry time after the burst. The data shown in Figures 7 and 8 can be used as follows. Suppose a survivor returns to within 500 m from

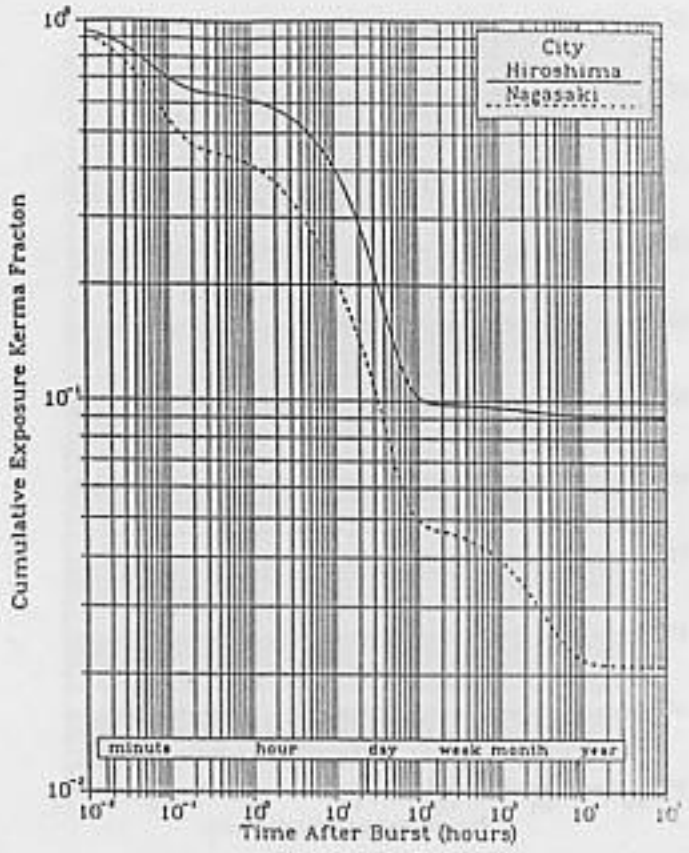


*Figure 8. Cumulative exposure kerma fraction versus time after burst Hiroshima and Nagasaki*

the hypocenter at Hiroshima the day after the burst and remains in the general vicinity for two days. From Figure 7, the infinite stay kerma at 500 m ground range in Hiroshima is about 20 rad. From Figure 8, an entry time at one day with an infinite stay would result in accumulating 25% of this infinite stay kerma or 5 rad. But, upon leaving after the third day, the subject is no longer exposed to about 12% of this infinite stay kerma. Thus, this survivor's kerma would have been approximately (0.25 - 0.12) × 20 = 2.6 rad.

It is difficult to assign an uncertainty to associate with the kerma rates presented here. Certainly, the uncertainty at Nagasaki is larger due to the complicating delayed neutron contribution. It is also true that any uncertainty ought to be time dependent due to the fact that an unkown element or one not considered in the calculations can change the time-dependent kerma rate behavior over some unknown time regime. And if localized elemental soil compositions are considered, then any uncertainty ought also to reflect such unknowns. However, given the soil compositions, the neutron fluence distributions in the ground, the activation cross sections, and the gamma-ray transport out of the ground, we estimate that the free-field kerma rates due to soil activation in Hiroshima have a 25% calculational uncertainty while those near (<1000 m) the hypocenter at Nagasaki have 50% decreasing to 25% beyond 1500 m.

**Conclusions**

There are several conclusions concerning the calculated kermas due to soil activation at Hiroshima and Nagasaki as presented. With a caveat concerning soil trace element com-

positions, it appears that the initial kerma rates were larger at Hiroshima until about one week after the bombings. From then on, those at Nagasaki were larger. Of course, localized elemental variations in soil composition would change this conclusion. Additionally, remembering the assumptions made in estimating the delayed neutron fluences in the ground, this contribution, while negligible at Hiroshima, increases the kerma rates near the hypocenter in Nagasaki by a factor of two. The most important conclusion is that while the kermas calculated and discussed here are relatively small, they are nevertheless nonnegligible, especially as it concerns possible exposure to control survivors used in radiation risk analysis.

## References

1. Roussin, R. W., Muir, D. W., and Battat M. E., 1978. Informal Notes Describing DLC-33/Montage-400. Oak Ridge, TN: Oak Ridge National Laboratory, Radiation Shielding Information Center Data Library Collection DLC-33C : Montage-400.
2. Engle, W. W. Jr., 1967. Users Manual for ANISN - A One-Dimensional Discrete Ordinates Transport Code with Anisotropic Scattering. Oak Ridge, TN: Oak Ridge Gaseous Diffusion Plant, report K-1693.